Dear Author

Here are the proofs of your article.

- You can submit your corrections **online,** via **e-mail** or by **fax**.
- For **online** submission please insert your corrections in the online correction form. Always indicate the line number to which the correction refers.
- You can also insert your corrections in the proof PDF and **email** the annotated PDF.
- For **fax** submission, please ensure that your corrections are clearly legible. Use a fine black pen and write the correction in the margin, not too close to the edge of the page.
- Remember to note the **journal title**, **article number**, and **your name** when sending your response via e-mail or fax.
- **Check** the metadata sheet to make sure that the header information, especially author names and the corresponding affiliations are correctly shown.
- **Check** the questions that may have arisen during copy editing and insert your answers/corrections.
- **Check** that the text is complete and that all figures, tables and their legends are included. Also check the accuracy of special characters, equations, and electronic supplementary material if applicable. If necessary refer to the *Edited manuscript*.
- The publication of inaccurate data such as dosages and units can have serious consequences. Please take particular care that all such details are correct.
- Please **do not** make changes that involve only matters of style. We have generally introduced forms that follow the journal's style.
- Substantial changes in content, e.g., new results, corrected values, title and authorship are not allowed without the approval of the responsible editor. In such a case, please contact the Editorial Office and return his/her consent together with the proof.
- If we do not receive your corrections **within 48 hours**, we will send you a reminder.
- Your article will be published **Online First** approximately one week after receipt of your corrected proofs. This is the **official first publication** citable with the DOI. **Further changes are, therefore, not possible.**
- The **printed version** will follow in a forthcoming issue.

Please note

After online publication, subscribers (personal/institutional) to this journal will have access to the complete article via the DOI using the URL:

`http://dx.doi.org/10.1007/s00704-011-0480-2`

If you would like to know when your article has been published online, take advantage of our free alert service. For registration and further information, go to: http://www.springerlink.com.

Due to the electronic nature of the procedure, the manuscript and the original figures will only be returned to you on special request. When you return your corrections, please inform us, if you would like to have these documents returned.

AUTHOR'S PROOF!

Metadata of the article that will be visualized in OnlineFirst

1	Article Title	**Radiation balance at the surface in the city of São Paulo, Brazil: diurnal and seasonal variations**	
2	Article Sub- Title		
3	Article Copyright - Year	**Springer-Verlag 2011 (This will be the copyright line in the final PDF)**	
4	Journal Name	Theoretical and Applied Climatology	
5	Corresponding Author	Family Name	**Oliveira**
6		Particle	**de**
7		Given Name	**Amauri Pereira**
8		Suffix	
9		Organization	University of São Paulo
10		Division	Group of Micrometeorology, Department of Atmospheric Sciences, Institute of Astronomy, Geophysics and Atmospheric Sciences
11		Address	Rua do Matão, 1226, São Paulo 05508.090, São Paulo, Brazil
12		e-mail	apdolive@usp.br
13	Author	Family Name	**Ferreira**
14		Particle	
15		Given Name	**Mauricio Jonas**
16		Suffix	
17		Organization	University of São Paulo
18		Division	Group of Micrometeorology, Department of Atmospheric Sciences, Institute of Astronomy, Geophysics and Atmospheric Sciences
19		Address	Rua do Matão, 1226, São Paulo 05508.090, São Paulo, Brazil
20		e-mail	
21	Author	Family Name	**Soares**
22		Particle	
23		Given Name	**Jacyra**
24		Suffix	
25		Organization	University of São Paulo

26		Division	Group of Micrometeorology, Department of Atmospheric Sciences, Institute of Astronomy, Geophysics and Atmospheric Sciences
27		Address	Rua do Matão, 1226, São Paulo 05508.090, São Paulo, Brazil
28		e-mail	
29	Author	Family Name	**Codato**
30		Particle	
31		Given Name	**Georgia**
32		Suffix	
33		Organization	University of São Paulo
34		Division	Group of Micrometeorology, Department of Atmospheric Sciences, Institute of Astronomy, Geophysics and Atmospheric Sciences
35		Address	Rua do Matão, 1226, São Paulo 05508.090, São Paulo, Brazil
36		e-mail	
37	Author	Family Name	**Bárbaro**
38		Particle	
39		Given Name	**Eduardo Wilde**
40		Suffix	
41		Organization	University of São Paulo
42		Division	Group of Micrometeorology, Department of Atmospheric Sciences, Institute of Astronomy, Geophysics and Atmospheric Sciences
43		Address	Rua do Matão, 1226, São Paulo 05508.090, São Paulo, Brazil
44		e-mail	
45	Author	Family Name	**Escobedo**
46		Particle	
47		Given Name	**João Francisco**
48		Suffix	
49		Organization	State University of São Paulo
50		Division	Department of Natural Resources, School of Agronomic Sciences
51		Address	Botucatu , São Paulo, Brazil
52		e-mail	

53	Schedule	Received	7 January 2011
54		Revised	
55		Accepted	23 June 2011

56 Abstract

The main goal of this work is to describe the diurnal and seasonal variations of the radiation balance components at the surface in the city of São Paulo that are described based on observations carried out during 2004. Monthly average hourly values indicate that the amplitudes of the diurnal cycles of net radiation (*Q**), downwelling and upwelling shortwave radiation (SW_{DW}, SW_{UP}), and longwave radiations (LW_{DW}, LW_{UP}) in February were, respectively, 37%, 14%, 19%, 11%, and 5% larger than they were in August. The monthly average daily values indicate a variation of 60% for *Q**, with a minimum in June and a maximum in December; 45% for SW_{DW}, with a minimum in May and a maximum in September; 50% for SW_{UP}, with a minimum in June and a maximum in September; 13% for LW_{DW}, with a minimum in July and a maximum in January; and 9% for LW_{UP}, with a minimum in July and a maximum in February. It was verified that the atmospheric broadband transmissivity varied from 0.36 to 0.57; the effective albedo of the surface varied from 0.08 to 0.10; and the atmospheric effective emissivity varied from 0.79 to 0.92. The surface effective emissivity remained approximately constant and equal to 0.96. The albedo and surface effective emissivity for São Paulo agreed with those reported for urban areas in Europe and North America cities. This indicates that material and geometric effects on albedo and surface emissivity in São Paulo are similar to ones observed in typical middle latitudes cities. On the other hand, it was found that São Paulo city induces an urban heat island with daytime maximum intensity varying from 2.6°C in July (16:00 LT) to 5.5°C in September (15:00 LT). The analysis of the radiometric properties carried out here indicate that this daytime maximum is a primary response to the seasonal variation of daily values of net solar radiation at the surface.

57 Keywords separated by ' - '

58 Foot note information

Theor Appl Climatol
DOI 10.1007/s00704-011-0480-2

ORIGINAL PAPER

Radiation balance at the surface in the city of São Paulo, Brazil: diurnal and seasonal variations

Mauricio Jonas Ferreira · Amauri Pereira de Oliveira · Jacyra Soares · Georgia Codato · Eduardo Wilde Bárbaro · João Francisco Escobedo

Received: 7 January 2011 / Accepted: 23 June 2011

Abstract The main goal of this work is to describe the diurnal and seasonal variations of the radiation balance components at the surface in the city of São Paulo that are described based on observations carried out during 2004. Monthly average hourly values indicate that the amplitudes of the diurnal cycles of net radiation (Q^*), downwelling and upwelling shortwave radiation (SW_{DW}, SW_{UP}), and longwave radiations (LW_{DW}, LW_{UP}) in February were, respectively, 37%, 14%, 19%, 11%, and 5% larger than they were in August. The monthly average daily values indicate a variation of 60% for Q^*, with a minimum in June and a maximum in December; 45% for SW_{DW}, with a minimum in May and a maximum in September; 50% for SW_{UP}, with a minimum in June and a maximum in September; 13% for LW_{DW}, with a minimum in July and a maximum in January; and 9% for LW_{UP}, with a minimum in July and a maximum in February. It was verified that the atmospheric broadband transmissivity varied from 0.36 to 0.57; the effective albedo of the surface varied from 0.08 to 0.10; and the atmospheric effective emissivity varied from 0.79 to 0.92. The surface effective emissivity remained approximately constant and equal to 0.96. The albedo and surface effective emissivity for São Paulo agreed with those reported for urban areas in Europe and North America cities. This indicates that material and geometric effects on albedo and surface emissivity in São Paulo are similar to ones observed in typical middle latitudes cities. On the other hand, it was found that São Paulo city induces an urban heat island with daytime maximum intensity varying from 2.6°C in July (16:00 LT) to 5.5°C in September (15:00 LT). The analysis of the radiometric properties carried out here indicate that this daytime maximum is a primary response to the seasonal variation of daily values of net solar radiation at the surface.

Symbol list

ASDC	Atmospheric Sciences Data Center
UHI	Urban heat island
NASA	National Aeronautics and Space Administration
MRSP	Metropolitan region of São Paulo
SRB	Surface radiation balance
USP	University of São Paulo
WMO	World Meteorological Organization
ECOVIAS	Company of Management of the Imigrante's Thruway
IAG	Institute of Astronomy, Geophysics and Atmospheric Sciences, micrometeorological platform
PEFI	Meteorological station of IAG
UBL	Urban boundary layer
$\Delta T_{u\text{-}r}$	Air temperature difference between urban and adjacent rural areas
Q^*	Net radiation at the surface (W m^{-2})
SW_{DW}	Incoming shortwave radiation at the surface (W m^{-2})
SW_{UP}	Outgoing shortwave radiation at the surface (W m^{-2})
SW_{TOP}	Extraterrestrial solar radiation (W m^{-2})

M. J. Ferreira · A. P. de Oliveira (✉) · J. Soares · G. Codato · E. W. Bárbaro
Group of Micrometeorology, Department of Atmospheric Sciences, Institute of Astronomy, Geophysics and Atmospheric Sciences, University of São Paulo,
Rua do Matão, 1226,
05508.090 São Paulo, São Paulo, Brazil
e-mail: apdolive@usp.br

J. F. Escobedo
Department of Natural Resources, School of Agronomic Sciences, State University of São Paulo,
Botucatu, São Paulo, Brazil

LW_{DW}	Incoming longwave radiation at the surface (W m^{-2})
LW_{UP}	Outgoing longwave radiation at the surface (W m^{-2})
SW*	Net shortwave radiation at the surface (W m^{-2})
LW*	Net longwave radiation at the surface (W m^{-2})
σ	Stefan–Boltzmann constant (5.67×10^{-8} K^{-4}W m^{-2})
T_{AIR}	Air temperature (screen level=1.5 m)
T_{SUR}	Surface temperature
Γ	Broadband atmospheric transmissivity
α	Surface effective albedo
ε_{ATM}	Atmospheric effective emissivity
ε_{SUR}	Surface effective emissivity

1 Introduction

According to the United of Nations, 85% of the Brazilian population lived in urban areas in 2005, and this figure is expected to have increased to approximately 87% in 2010. In developed countries, the urban fraction of the population is expected to grow from 75% in 2005 to approximately 78% in 2010 (Cohen 2004; Masson 2006; UN 2007). If confirmed, the urban population growth may intensify the substitution of naturally and artificially vegetated surfaces by urban land use, favoring the formation of several microclimates that may differ considerably from the climate of the original and adjacent areas (Arnfield 2003; Kalnay and Cai 2003; Collier 2006; Trusilova et al. 2009).

In general, urban surfaces absorb and retain more energy than rural or naturally vegetated surfaces because their geometry favors absorption of radiation by increasing the interaction between radiation and the surface as a consequence of multiple reflections and emissions (geometric effect). In addition, large portions of the urban surfaces are made of materials such as concrete or asphalt that are characterized by albedo and emissivity smaller than naturally or artificially vegetated surfaces (the material effect; Landsberg 1981). Moreover, urban areas have an extra input of energy due to the anthropogenic energy flux associated with vehicular and stationary sources (Grimmond 1992; Sailor and Lu 2004; Ferreira 2010). As a consequence of all these inputs of energy, the urban climate is characterized by the urban heat island ($\Delta T_{u\text{-}r}$>0).

To understand the impact of urban growth on the local climate, it is necessary to estimate objectively the exchange of energy, momentum, and mass between the atmosphere and the surface. The radiation balance at the surface is one of the most important parts of the energy balance because it defines the main input of energy at the interface between the atmosphere and the surface (White et al. 1978). The radiation balance at the surface can be estimated by adding the incoming and outgoing fluxes of shortwave and long-wave radiation at the surface as follows:

$$Q^* = SW_{DW} + SW_{UP} + LW_{DW} + LW_{UP}, \tag{1}$$

where Q^* is the net radiation; SW_{DW} and SW_{UP} are, respectively, the incoming and outgoing shortwave radiations; and LW_{DW} and LW_{UP} are, respectively, the incoming and outgoing longwave radiations. Hereafter, downward fluxes are negative, and upward fluxes are positive.

At the surface, these radiation components can be observed directly using a set of radiometers (in situ measurements) or indirectly using empirical expressions based on meteorological parameters observed regularly by surface weather stations, specifically screen air temperature, screen air relative humidity, and cloud cover and type (Offerle et al. 2003; Diak et al. 2004; Oke 2004). Satellite estimates can also provide accurate information about all components of the radiation balance at the surface for urban areas with good spatial resolution and temporal continuity. However, in situ observations are preferred in urban areas because satellite measurements require frequent calibration to ground-based measurements and are strongly affected by cloud cover, which is a significant issue in tropical latitudes (Garratt and Prata 1996; Gupta et al. 1999; Hinkelman et al. 2009).

Net radiation at the surface in urban areas varies little compared to adjacent rural or naturally vegetated (non-urban) areas; nevertheless, when the four components indicated in Eq. 1 are considered individually over urban areas, they may differ considerably from their counterparts in non-urban areas due to differences in the surface emissivity, albedo, thermal properties of the substrate (thermal capacity, conductivity, and admittance) and atmospheric transmissivity and emissivity. In urban areas, the incoming and outgoing solar radiations at the surface are systematically smaller than they are in adjacent rural areas, whereas the incoming and outgoing longwave radiations over urban areas are larger than they are over adjacent non-urban areas. Observations indicate that the combined effects of solar radiation components (incoming and outgoing) and longwave radiation components (incoming and outgoing) yield values of net radiation at the surface over urban areas that are slightly larger than they are over adjacent non-urban areas located in middle and high latitudes and surround by vegetated areas (Oke 1974, 1982; White et al. 1978; Landsberg 1981; Estournel et al. 1983; Schmid et al. 1991).

Very often, the presence of vegetation decreases the net radiation at the surface over urban areas mainly because the albedo of vegetated surfaces is larger than that of urban surfaces (vegetation effect; Brest 1987). However, variations in the net radiation due to the vegetation effect depend strongly on the contrast between urban and non-urban landscapes, mainly in vegetation height and soil moisture content (soil moisture effect). In some cases, the presence of vegetation combined with irrigation may unexpectedly increase the net radiation at the surface over urban areas (Grimmond et al. 1996). In other words, the complexity of urban surfaces makes it difficult to infer general rules for net radiation that can be generalized for all kinds of cities and climates. So it is more appropriate to look at each of the individual components of the radiation balance and at the corresponding radiometric properties of the atmosphere and surface that determine their behavior. Therefore, hereafter, the downwelling solar radiation at the surface (SW_{DW}) will be linked to the atmospheric broadband transmissivity at the surface (Γ); the upwelling solar radiation at the surface (SW_{UP}) to the effective albedo of the surface (α), the downwelling longwave radiation at the surface (LW_{DW}) to the effective atmospheric emissivity at the surface (ε_{ATM}), and the upwelling longwave radiation at the surface (LW_{UP}) to the effective emissivity of the surface (ε_{SUR}).

As indicated in the brief review above, most of the information available about radiation balance at the surface is based on observations carried out in middle and high latitude cities. However, it is very difficult to systematize the available information because of the complexity associated with all the physical processes that determine the radiation balance at the surface over urban areas. Moreover, very little is known about the radiation balance at the surface in urban areas located in subtropical regions.

Therefore, the main objective of this work is to describe the diurnal and seasonal variation of the radiation balance at the surface in the metropolitan region of São Paulo (MRSP), Brazil. This goal will be pursued using in situ observations of net radiation and its four components carried out continuously on the micrometeorological platform located at the top of a building located in the city of São Paulo. The description will include four bulk radiometric properties: atmospheric broadband transmissivity, surface effective albedo, atmospheric effective emissivity, and surface effective emissivity. These parameters offer simple and physically sound information that can be used to characterize urban effects on the radiation balance components and for comparison to other urban regions. In this paper, the basic features of these four radiometric bulk parameters for urban surfaces are reviewed in Section 2. Observations used in this work and a detailed analysis of temporal and spatial representativeness of these observations are described in the Section 3. Section 4 describes the time evolution (diurnal and seasonal) of the radiation balance at the surface. The bulk radiometric properties are shown in Section 5. Relationship between radiation balance at the surface and UHI in São Paulo city are explored in Section 6. Major finds are summarized in Section 7.

2 Basic features of the radiation balance in urban surfaces

The atmospheric broadband transmissivity at the surface is the ratio of the downwelling solar radiation at the surface to the solar radiation at the top of the atmosphere ($\Gamma=SW_{DW}/SW_{TOP}$). It varies in time and space depending on the atmospheric water vapor content, aerosol load, trace gas concentrations (such as CO_2, CH_4, NO_2, and O_3), and cloud amount, type, and altitude. Over urban regions, the variation is observed as a reduction in the downwelling solar radiation at the surface with respect to the adjacent non-urban areas due to the reduction of the atmospheric broadband transmissivity caused by the presence of larger concentrations of gases and aerosols in the urban atmosphere associated with vehicular and other urban air pollution sources (pollution effect; Rouse et al. 1973; Peterson and Flowers 1977; Peterson and Stoffel 1980; Estournel et al. 1983; Oke 1988; Stanhill and Kalma 1995; Oliveira et al. 1996, 2002; Jáuregui and Luyando 1999; Codato et al. 2008).

Table 1 indicates that in some polluted urban areas, the reduction of SW_{DW} reaches as much as 22% compared to adjacent rural areas due to pollution, mainly particulate matter. Under clear sky conditions, reductions on the order of 21% to 22% in the SW_{DW} were observed over the Mexico City in comparison to non-urban areas in the vicinity. These reductions were also attributed to high levels of particulate matter (Jáuregui and Luyando 1999). Similar reductions due to air pollution were observed in the 5-min average values of beam radiation at the surface in the city of São Paulo during clear days (Oliveira et al. 1996). Diminutions between 5% and 13.4% in the monthly average hourly values of global solar radiation at the surface in São Paulo were observed during clear sky days, also in association with air pollution (Oliveira et al. 2002). On the regional scale (approximately 200 km), global solar radiation in São Paulo showed similar attenuation due to urban air pollution and the regional pattern of moisture (Codato et al. 2008).

The upwelling solar radiation at the surface depends on the surface effective albedo ($\alpha=-SW_{UP}/SW_{DW}$), which, in the case of urban areas, depends on the combination of the materials and the geometric effects. Urban materials (such as asphalt, concrete, and tile) and canopy geometry make the albedo over urban areas smaller than it is over surfaces covered by natural materials (such as those found in rural, forest or desert areas; Sailor and Fan 2002). As observed for all types of surfaces, the effective surface albedo over

Table 1 Some typical variations in the incoming shortwave radiation at the surface in urban areas and their main causes

City	Latitude, longitude, altitude	Reduction of SW_{DW}	Main cause
Hamilton, Canada (Rouse et al. 1973)	43°16′ N, 79°54′ W, 106 m	12%	Pollution
St. Louis, MO, USA (Peterson and Stoffel 1980)	38°38′ N, 90°11′ W, 142 m	3–4%	Pollution
Toulouse, France (Estournel et al. 1983)	43°36′ N, 1°26′ E, 166 m	3.5%	Pollution
Hong Kong, China (Stanhill and Kalma 1995)	22°19′ N, 114°10′ E, 65 m	1.06% per year	Cloud and pollution
Mexico City, Mexico (Jáuregui and Luyando 1999)	19°36′ N, 98°57′ W, 2,235 m	21% (dry season) 22% (wet season)	Pollution (aerosol)
São Paulo, Brazil (Oliveira et al. 1996)	23°33′ S, 46°38′ W, 792 m	18%	Pollution (aerosol)
São Paulo, Brazil (Oliveira et al. 2002)	23°33′ S, 46°38′ W, 792 m	10–12%	Pollution (aerosol)
São Paulo, Brazil (Codato et al. 2008)	23°33′ S, 46°38′ W, 792 m	13.4% (June), 5.0% (December)	Pollution (aerosol) and moisture

urban areas decreases with the sun elevation, showing minima in the middle of the day (diurnal variation), in the summer (seasonal variation), and at low latitudes (latitudinal variation). The diurnal, seasonal, and latitudinal variations of the surface albedo associated with the sun elevation are strongly affected by the presence of clouds (cloud effect). According to Yang (2006), only the beam component of the solar radiation field at the surface shows sun elevation effects on the albedo of the surface. The attenuation of the beam component induced by clouds reduces the effects associated with the elevation of the sun. The presence of vegetation in the cities increases the effective albedo mainly because the vegetation reflects a significant fraction of the near infrared (0.7 to 3.0 μm) portion of the solar radiation spectrum (Brest 1987), and this part of the spectrum contributes approximately 50% of the global solar radiation at the surface (Escobedo et al. 2011).

Observations indicate that in urban areas located at middle latitudes and for snow-free conditions, the surface albedo ranges from 0.10 to 0.27, with an average of 0.15 (Oke 1988). In this case, the surface albedo shows a maximum in the summer and a minimum during the winter (Table 2). This seasonal variation has been observed in St. Louis, MO, USA by White et al. (1978) and by Vukovich (1983); in Hartford, CT, USA by Brest (1987); and in Ibadan, Nigeria by Adebayo (1990). It is due mainly to the presence of vegetation (vegetation effect), which increases the albedo during summer in urban areas located at middle latitudes (Table 2). The vegetation effect in these urban areas seems to be strong enough to overcome the geometric effect, which tends to decrease the albedo during summer, when the sun elevation is higher (seasonal variation). In the presence of snow, the surface albedo in urban areas shows a seasonal variation with a minimum in the summer and a

Table 2 Seasonal variations in the surface albedo over urban areas and differences between urban and rural areas

Q3

City	Latitude, longitude, altitude	Urban [rural] albedo		Main cause
		Summer	Winter	
Urban/rural differences and seasonal variations—snow-free conditions				
St. Louis[a], MO, USA (White et al. 1978)	38°38′ N, 90°11′ W, 142 m	0.12 [0.16]	+	Vegetation effect
St. Louis[b], MO, USA (Vukovich 1983)	38°38′ N, 90°11′ W, 142 m	0.16 [0.19]	0.09 [0.10]	Vegetation effect
Hartford[b], CT, USA (Brest 1987)	41°46′ N, 72°45′ W, 22 m	0.12 [0.19]	0.08 [0.07]	Vegetation effect
Ibadan[c], Nigeria, (Adebayo 1990)	7°24′ N, 3°55′ E, 234 m	0.15 [0.17]	0.14 [0.16]	Vegetation effect
Seasonal variations in the presence of snow				
Chicago[d], IL, USA, (Offerle et al. 2003)	41°50′ N, 87°37′ W 177 m.	0.16	0.23	Geometric an snow effects
Łódz[d], Poland (Offerle et al. 2003)	51°47′ N, 19°28′ E, 200 m.	0.07	0.09	Geometric and snow effects

+ not available

[a] Aircraft measurements

[b] Satellite estimates

[c] In situ measurements

[d] In situ modeling

JrnlID 704_ArtID 480_Proof# 1 - 01/07/2011

Q1

maximum in the winter. This effect has been observed in Chicago, IL, USA by Offerle et al. (2003) and, with less intensity, in Łódz, Poland by Offerle et al. (2003). The presence of snow is the main reason for the increase of albedo in the winter in these cities, even though the effective albedo of the surface is expected to increase in the winter, when the sun elevation is smaller than it is in the summer (Table 2).

The downwelling longwave radiation at the surface, LW_{DW}, in the urban canopy (Table 3) is determined by cloud cover, sky obstruction, thermal and moisture stratification of the lowest layers, and air pollution load (Rouse et al. 1973; Welch and Zdunkowski 1976; Dalrymple and Unsworth 1978; Estournel et al. 1983; Jonsson et al. 2006). The presence of air pollution and urban heat island (UHI) increases LW_{DW} in urban areas compared to adjacent rural areas. These effects are amplified by the presence of moisture and vary with the geographic position (Oke 1988). The effective atmospheric emissivity, $\varepsilon_{ATM} = -LW_{DW}/\sigma T_{AIR}^4$, where σ is the Stefan–Boltzmann constant and T_{AIR} is the air temperature at screen level, indicates the capacity of lower layers of the atmosphere to emit downward radiation to the surface as a consequence of their composition and thermal stratification (Rouse et al. 1973; Oke 1988; Niemelä et al. 2001; Offerle et al. 2003; Bárbaro et al. 2010).

The surface temperature and effective emissivity allow quantification of the total amount of upwelling longwave radiation at the surface (LW_{UP}). However, measurements of surface temperature over urban areas are rather cumbersome because of the complexity of the buildings and other urban structures and the variety of urban materials. In general, the surface temperature in urban areas is higher than in the adjacent rural areas during most of the day and the year (White et al. 1978; Sellers et al. 1990; Voogt and Oke 1997; Moriwaki and Kanda 2004).

It is observed that effective emissivity of a natural surface varies seasonally due to surface cover (material and geometry of the canopy) and surface moisture (Jin and Liang 2006; Mira et al. 2007). Estimates of the surface effective emissivity, $\varepsilon_{SUR} = LW_{UP}/\sigma T_{SUR}^4$, where T_{SUR} is the surface temperature, are indicated in Table 4 for different urban regions. In general, the surface effective emissivity in urban areas is slightly lower than it is in the adjacent rural areas. This behavior is due to a trapping effect caused by canyon geometry.

Over urban areas, the surface effective emissivity varies between 0.85 and 0.96, averaging 0.95 (Oke 1988). Some other studies have indicated surface effective emissivity ranging from 0.87 (Balling and Brazel 1988) to 0.97 (Dousset 1989; Henry et al. 1989). In a recent review, Voogt and Oke (2003) indicated that for most urban areas, the surface effective emissivity values vary between 0.92 and 0.95.

3 Site and observations

The city of São Paulo is located 60 km from the Atlantic Ocean and belongs to a conurbation of 39 cities (Fig. 1) where the largest industrial park of South America is located. The surface area is 8051 km^2, and there are more than 19.6 million inhabitants (IBGE 2008). The city has undergone extensive economical development in recent decades, resulting in an intense and disordered population growth. It suffers from chronic environmental problems, mainly air pollution caused by more than seven million vehicles and 30,000 industries (CETESB 2009).

3.1 Observations

The seasonal and diurnal variations of the radiation balance at the surface are based on in situ observations in the city of São Paulo carried out during 2004 (Fig. 1; Table 5). The data are 5-min average values of net radiation and shortwave and longwave incoming and outgoing radiation components at the surface at the IAG (site 1). To complement the

Table 3 Variations of the incoming longwave radiation at the surface (LW_{DW}) in urban areas Q4

City	Latitude, longitude, altitude	Increase in LW_{DW}	Cause
Hamilton, Canada (Rouse et al. 1973)	43°16′ N, 79°54′ W, 106 m	23.5% (daily values)	Pollution (aerosol)
Mainz, Germany (Welch and Zdunkowski 1976)	49°58′ N, 8°9′ E, 231 m	10% (RH=40%) 35% (RH=90%)	Pollution and moisture
Sutton Bonington, England (Dalrymple and Unsworth 1978)	52°50′ N, 1°15′ W, 65 m	20 Wm^{-2}	Pollution (aerosol)
Toulouse, France (Estournel et al. 1983)	43°36′ N, 1°26′ E, 166 m	15 Wm^{-2} ($\Delta T_{u\text{-}r}$=5°C) 25 Wm^{-2} ($\Delta T_{u\text{-}r}$=6°C)	UHI
Dar es Salaan, Tanzania (Jonsson et al. 2006) Ouagadougou, Burkina Faso (Jonsson et al. 2006) Gaborone, Botswana (Jonsson et al. 2006)	6°51′ S, 39°18′ E, 0 m 12°20′ N, 1°40′ W, 300 m 24°40′ S, 25°55′ E 1,000 m	$LW_{DW\ Dar\ es\ Salaan}$ > $LW_{DW\ Ouagadougou}$ > $LW_{DW\ Gaborone}$	Altitude

Table 4 Surface emissivity estimated for urban areas

City	Latitude, longitude, altitude	ε_{SUR}	Observation period (year/year day)
Chicago, IL, USA (Offerle et al. 2003)	41°50′ N, 87°37 W, 177 m	0.93	1992/198–1993/158
Los Angeles, CA, USA (Offerle et al. 2003)	34°03′ N, 118°15′ W, 100 m	0.94	1993/225–1994/206
Łódz, Poland (Offerle et al. 2003)	51°47′ N, 19°28′ E, 200 m	0.92	2001/001–365

characterization of the radiation balance at the surface, the following data were also used: hourly values of surface and air temperature observed at the climatological surface station located at PEFI (site 2), hourly values of air temperature observed at screen level at five surface stations belonging to the air pollution network of CETESB (sites 3 through 7) and at eight weather stations operated by ECOVIAS (sites 8–15), and 3-h average values of net radiation and shortwave and longwave incoming and outgoing radiation components at the surface estimated at four grid points by the SRB project (sites 16–19). These complementary data were also collected in 2004.

In the IAG, measurements of radiation were carried out on the micrometeorological platform located at the Institute of Astronomy, Geophysics and Atmospheric Sciences of the University of São Paulo (Figs. 1 and 2). The measurements of net radiation and incoming and outgoing solar and longwave radiation at the surface were obtained using a net radiometer model CNR1 from Kipp–Zonen. The accuracy of these sensors is ±10%. These measurements were taken with a sampling frequency of 0.2 Hz and stored as 5-min averages. At the same location, measurements of air temperature using a thermistor from Väisälä were carried out simultaneously and with the same sampling frequency as were the solar and longwave radiation measurements described above. According to the manufacturer, the air temperature is measured with an accuracy of 0.1°C for a range of temperature between 0 and 40°C.

At the PEFI, measurements of surface and air temperature were carried out at the meteorological station of the Institute of Astronomy, Geophysics and Atmospheric Sciences of the University of São Paulo, located southeast of São Paulo city (site 2 in Fig. 1). Air temperatures were measured at the PEFI using a thermographer (Fuess). Surface temperature was measured with a geothermographer (Fuess). The accuracy of these sensors is 0.2°C.

The CETESB air pollution network stations provided hourly values of air temperature measured at screen level at five sites located within the urban limit of the city of São Paulo (sites 3–7 in Fig. 1). These stations are part of the surface air pollution network operated by CETESB, the State of São Paulo Environment Protection Agency. The accuracy of the temperature sensors is 0.1°C.

The ECOVIAS surface weather stations provided hourly values of the air temperature measured at screen level. Two weather stations operated by ECOVIAS (Company of Management of the Imigrante's Thruway) and located within the urban area of the city of São Paulo were selected. Hereafter, these sites will be referred to as ECOVIAS (labeled 8 and 9 in Fig. 1 and Table 5). Hourly

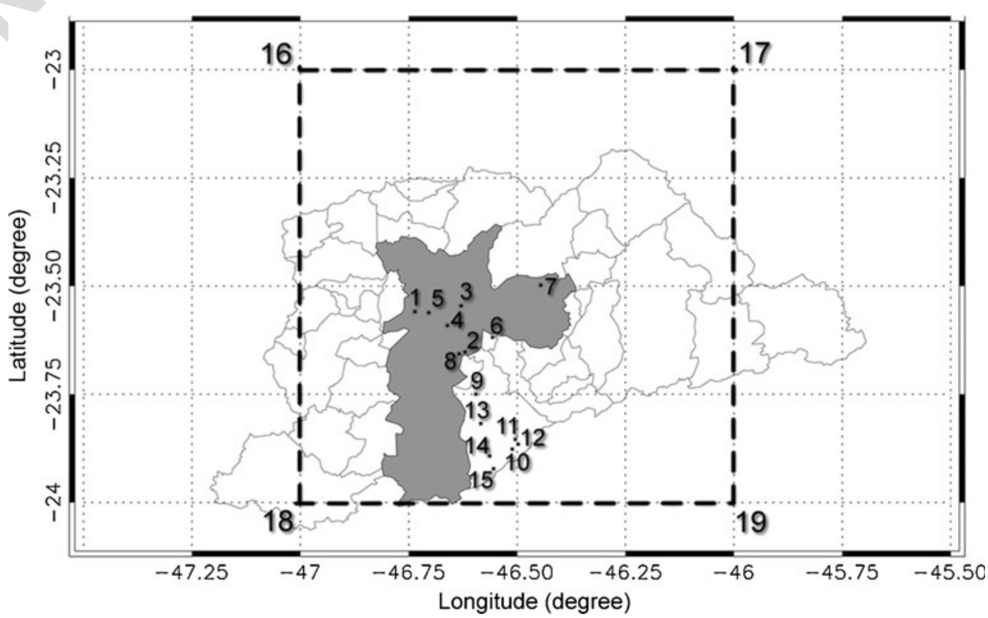

Fig. 1 Geographic position of the city of São Paulo (*gray area*). Measurements were carried out at the micrometeorological platform at the IAG (site 1), the PEFI climatological station (site 2), the CETESB air pollution station network (sites 3 through 7), the ECOVIAS weather station network (urban sites 8 and 9 and rural sites 10 through 15), and the SRB grid points (sites 16 through 19). *Dashed square* indicates the area represented by the SRB estimates

Table 5 Site and measurement information

Label (Fig. 1)	Site	Latitude; longitude; altitude	Parameter	Measurements frequency
1	IAG	23°33′34″ S; 46°44′01″ W; 744 m	Q^*, SW_{DW}, SW_{UP}, LW_{DW}, LW_{UP}, T_{AIR},	5 min
2	PEFI	23°39′05″ S; 46°37′21″ W; 730 m	T_{AIR}, T_{SUR}	Hourly
3	CETESB (Parque D. Pedro)	23°32′38″ S; 46°37′44″ W; 741 m	T_{AIR}	Hourly
4	CETESB (Ibirapuera)	23°35′28″ S; 46°39′36″ W; 755 m		
5	CETESB (Pinheiros)	23°33′40″ S; 46°42′07″ W; 728 m		
6	CETESB (São Caetano do Sul)	23°37′12″ S; 46°33′22″ W; 744 m		
7	CETESB (São Miguel Paulista)	23°29′53″ S; 46°26′38″ W; 780 m		
8	ECOVIAS (SP 160 km 12.1)	23°39′17″ S; 46°38′02″ W; 791 m	T_{AIR}	Hourly
9	ECOVIAS (SP 160 km 24.4)	23°44′56″ S; 46°35′46″ W; 769 m		
10	ECOVIAS (SP 40 km 2.0)	23°52′29″ S; 46°30′46″ W; 736 m		
11[a]	ECOVIAS (SP 150 km 38.8)	23°51′17″ S; 46°30′15″ W; 755 m		
12[a]	ECOVIAS (SP 150 km 40.1)	23°51′50″ S; 46°29′50″ W; 740 m		
13[a]	ECOVIAS (SP 160 km 32.3)	23°48′57″ S; 46°35′02″ W; 773 m		
14[a]	ECOVIAS (SP 160 km 40.5)	23°53′32″ S; 46°33′51″ W; 758 m		
15[a]	ECOVIAS (SP 160 km 44.4)	23°55′18° S; 46°33′19″ W; 736 m		
16	SRB	23° S; 47° W; 721 m	SW_{DW}, SW_{UP}, LW_{DW}, LW_{UP}, T_{SUR}	Every 3 h, daily, and monthly
17		23° S; 46° W; 758 m		
18		24° S; 47° W; 734 m		
19		24° S; 46° W; 0 m		

[a] Rural

values of air temperature at screen level measured in other six weather stations operated also by ECOVIAS and located over rural area at south of São Paulo (labeled 10 through 15 in Fig. 1 and Table 5) were used to estimate the intensity of UHI ($\Delta T_{\text{u-r}}$). The accuracy of the all these temperature sensors is 0.1°C.

The SRB radiation data consist of three-hourly, daily, and monthly values of incoming and outgoing shortwave and longwave radiation at the surface estimated from satellite data and provided by the SRB project of the Atmospheric Science Data Center of NASA (http://eosweb.larc.nasa.gov/HPDOCS/projects/rad_budg.html). These estimates have a spatial resolution of 1° of latitude by 1° of longitude and are derived from the vertical structure of the atmosphere and surface properties datasets combined with satellite observations and radiation transfer equations for shortwave and longwave radiation (Pinker and Laszlo 1992; Gupta et al. 1999; Stackhouse et al. 2000). The shortwave and longwave incoming and outgoing radiation at the surface provided by SRB had been validated by comparison with in situ measurements at several sites using Colorado State University general circulation model (Gupta et al. 1999). The results of these validations indicated that the largest mean bias error is on the order of 20 $\mathrm{W m^{-2}}$ for incoming longwave radiation. According to Gupta et al. (1999), the main sources of error are related to the uncertainty in the parameters of absorption and scattering of radiation in the atmosphere and to lack of information about cloud properties and aerosol extinction coefficients associated with local sources of air pollution.

3.2 Climate

According to Oliveira et al. (2002), the climate of São Paulo is typical of the subtropical regions of Brazil, being characterized by a dry winter from June to August and a wet summer from December to February.

The patterns of circulation in the city of São Paulo indicate a predominance of northeasterly flow, with velocities at the surface varying from 1.5 to 2.0 $\mathrm{m s^{-1}}$ during the nighttime and the morning. The winds are associated with the semi-stationary subtropical Atlantic high pressure system (South Atlantic High). During the afternoon and early night, the sea breeze penetrates the MRSP, shifting the wind direction to southeasterly and increasing the surface wind velocity to 2.5 to 3.0 $\mathrm{m s^{-1}}$. The large-scale pattern is frequently disturbed by the passage of cold fronts. The topography and land use also affect the wind in the MRSP. Blocking caused by buildings and channeling in canyons and valleys are the dominant effects when the winds are strong. When the winds are weak (<2 $\mathrm{m s^{-1}}$), the thermal circulation induced by mountain valley circulation plays a strong role in the local circulation (Oliveira et al. 2003).

According to Ferreira (2010), the anthropogenic energy flux at the surface in the city of São Paulo shows a diurnal

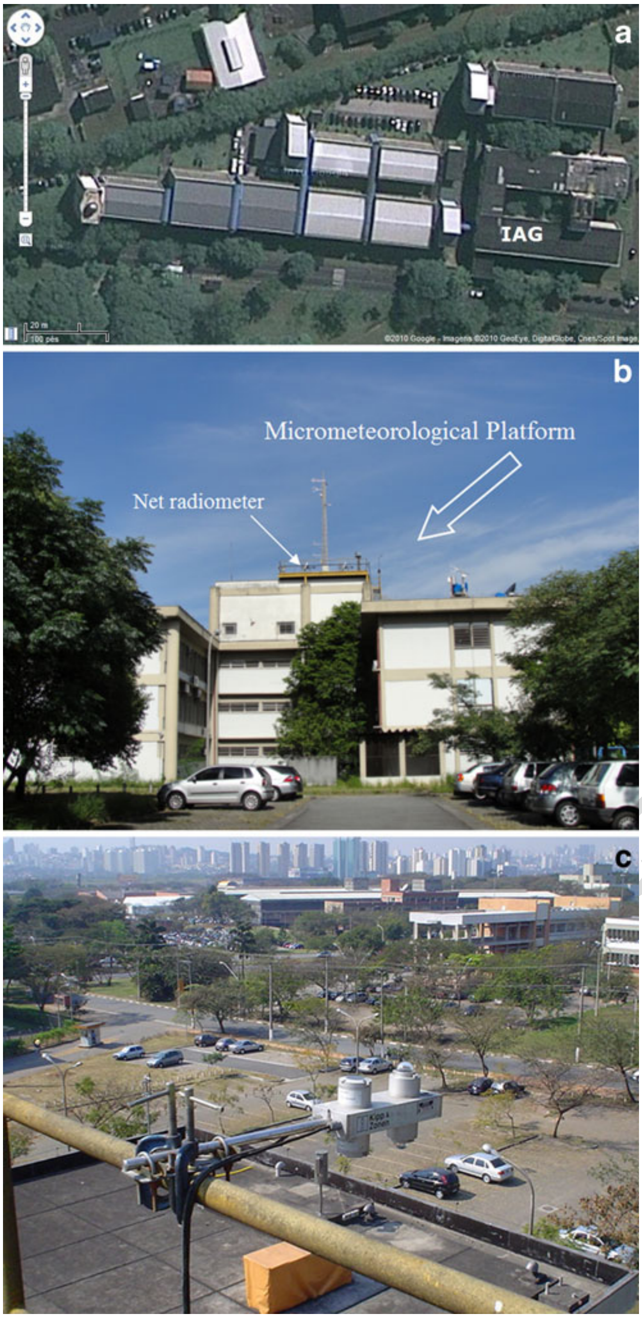

Fig. 2 **a** The IAG building, **b** the micrometeorological platform, and **c** the net radiometer. The land use of the University of São Paulo campus is classified as suburban. In **b**, the view is from the parking lot located east of the IAG building

evolution with maximum value on the order of 20 $\mathrm{W\,m^{-2}}$. The energy released by mobile sources is the dominant term, contributing 50% of the total anthropogenic energy flux. Stationary sources and human metabolism represent 41% and 9% of the anthropogenic heat, respectively. The annual value of the anthropogenic energy flux corresponds to approximately 11% of annual value of the net radiation at the surface, varying from 9% in December to 15% in June.

3.3 Climate conditions in São Paulo during 2004

Since the investigation carried out in this work is based on monthly average values of radiation components observed during 2004 at IAG, it is important to characterize how this year behaves with respect to the local climate. In this characterization, it will be considered as the reference of the climate of São Paulo city the seasonal variation given by the monthly averaged daily values of air temperature, relative humidity, and monthly accumulated values of precipitation estimated from hourly values of air temperature and relative humidity observed at PEFI (site 2 in Fig. 1). The hourly values of temperature and relative humidity were observed continuously during 75 years (from 1933 to 2008) and daily values of precipitation during 50 years (from 1958 to 2008). Details about these observations are given in the previous subsection and by Pereira Filho et al. (2007). Hereafter, these monthly average values will be referred as climatological normal of São Paulo city.

The seasonal variation of monthly averaged daily values of air temperature and relative humidity and monthly accumulate precipitation observed during 2004 at the IAG (Fig. 3, gray columns) indicates that the air temperature

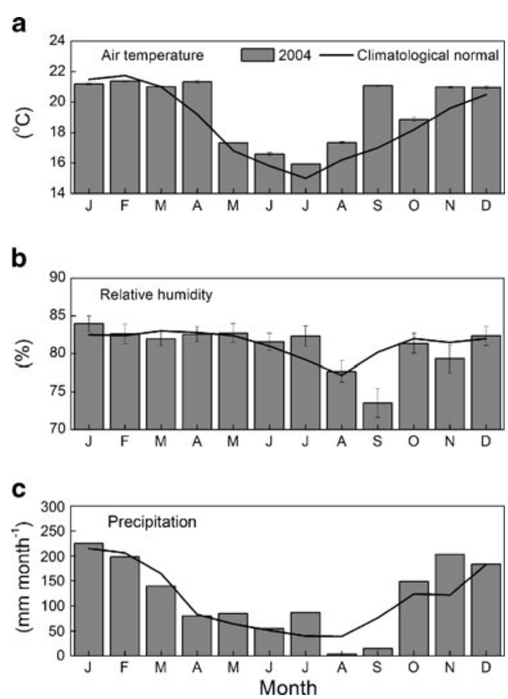

Fig. 3 Seasonal variation of **a** monthly average daily values of air temperature, **b** monthly average daily values of relative humidity, and **c** monthly accumulated precipitation in the city of São Paulo. Observations carried at the PEFI, between 1933 and 2008 for temperature and relative humidity and between 1958 and 2008 for rain, are indicated by *continuous line*. Observations carried out at the IAG during 2004 are indicated by *gray columns*. Statistical errors are indicated by vertical *bars*

reached a maximum of 21.3±0.5°C in February and a minimum of 15.9±0.5°C in July (Fig. 3a). The relative humidity reached a maximum of 84.3±1.7% in January and a minimum of 74.1±3.0% in September (Fig. 3b). In January occurred the maximum rainfall of 225 mm and in August the minimum of 3 mm (Fig. 3c). Therefore, the seasonal variation of temperature, relative humidity, and precipitation observed at the IAG during 2004 confirm the main climate features of São Paulo city described by Oliveira et al. (2002).

Comparatively to the climatological normal of São Paulo city, the air temperature observed at the IAG in 2004 is slightly higher during second semester (Fig. 3a, continuous line). The exception in 2004 is September. In this month, the temperature at IAG is much higher than normal. During this month in São Paulo, the precipitation was lower than normal (Fig. 3c) indicating that much more solar radiation has reached the surface. Excepted by July and September, the seasonal variation of relative humidity in 2004 does not show a significant discrepancy with respect to the climatological normal.

In general, the seasonal variation of temperature, relative humidity, and precipitation observed in during 2004 confirm the main climate features of São Paulo city, but they also display significant differences that will be important in the characterization of radiation balance and the radiometric properties at the surface of São Paulo in the next sections.

3.4 Representativeness

In this section, a statistical analysis is performed to compare measurements carried out at one point (net radiation components and air temperature measured at IAG and surface temperature measured at PEFI) with estimates representative of the urban area of São Paulo (satellite estimates of net radiation components corresponding to an area of 100×100 km) from the SRB project and spatially averaged air temperature and surface temperature using surface stations available in São Paulo (Table 5).

To assess objectively the agreement between one-point measurements and area estimates, the mean bias error (MBE), root mean square error (RMSE), determination coefficient (R^2), and test of variance (Snedecor and Cocharan 1989; Wilks 2006; Bárbaro et al. 2010) were used. Figures 4 and 5 display the dispersion diagrams and Table 6 the statistical parameters for all variables.

The dispersion diagrams in Fig. 4 compare all four components of net radiation measured at the IAG and estimated from SRB. There one can see that in the case of monthly average hourly values, there is a good agreement for all components, with MBE and RMSE on the order 11.2 and 45.2 $\mathrm{W\,m^{-2}}$ for SW_{DW}, 1.8 and 10.2 $\mathrm{W\,m^{-2}}$ for SW_{UP}, 1.2 and 8.6 $\mathrm{W\,m^{-2}}$ for LW_{DW}, and −11.1 and 14.1 $\mathrm{W\,m^{-2}}$ for LW_{UP}. These values are on the same order of magnitude as the ones obtained in previous analyses for other regions by Gupta et al. (1999) and Stackhouse et al. (2000). The

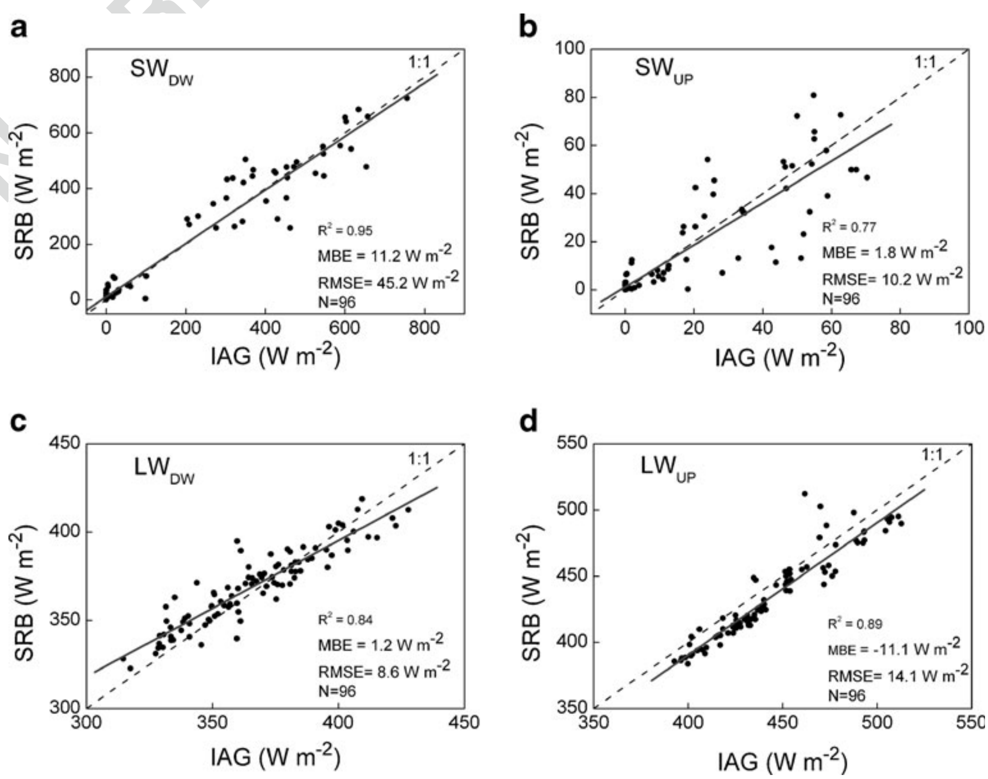

Fig. 4 Dispersion diagram comparing hourly values of incoming and outgoing shortwave and longwave radiation measured at the IAG and estimated by the SRB in 2004

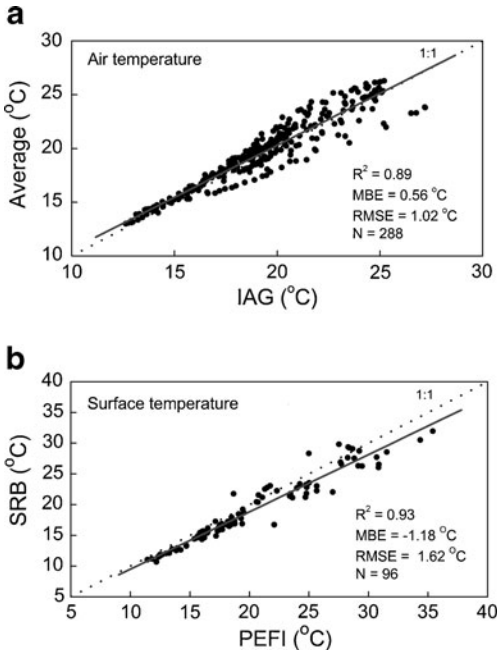

Fig. 5 Dispersion diagrams comparing hourly values of **a** air temperature measured at the IAG and the average over all the other sites in the city of São Paulo and **b** surface temperature measured at the PEFI and provided by the SRB project during 2004. The linear fit and the diagonal are indicated by *continuous* and *dotted lines*, respectively

coefficients of determination varied from 0.95 for SW_{DW} to 0.77 for SW_{UP}. The variance test for all four components shows that two data samples (one-point measurements and area estimates) presented an F value equal to 1.03 and a P value equal to 0.90 for SW_{DW}, an F value equal to 1.01 and a P value equal to 0.98 for SW_{UP}, an F value equal to 1.42 and a P value equal to 0.09 for LW_{DW}, and an F value equal to 0.89 and a P value equal to 0.56 for LW_{UP}. Therefore, it is possible to assume, at the 5% level, that the variances of monthly average hourly values of all four components of net radiation are not significantly different.

Similarly, the dispersion diagram in Fig. 5a compares air temperature measured at IAG and the average over all surface stations available in the city of São Paulo, including the IAG (sites 1 to 9 in Fig. 1 and Table 5). The diagram indicates that monthly average hourly values of air temperature measured at IAG show a good agreement with monthly average hourly values of air temperature based on the mean over all nine surface stations covering the entire city of São Paulo, with MBE and RMSE on the order 0.56°C and 1.02°C and R^2 equal to 0.89 (Table 6). The variance test shows that two data samples of T_{AIR} presented an F value equal to 0.96 and a P value equal to 0.70. Therefore, it is plausible to assume, at the 5% level, that the variances are not significantly different.

The comparison between surface temperatures measured at PEFI (site 2, Fig. 1; Table 5) and surface temperature provided by the SRB project are indicated in the dispersion diagram of Fig. 5b. The monthly average hourly values of surface temperature measured at PEFI agree very well with surface temperature estimated by the SRB project, with MBE and RMSE on the order −1.18°C and 1.62°C and a coefficient of determination equal to 0.93 (Table 6). The variance test on two data sets shows an F value equal to 1.04 and a P value equal to 0.84, indicating that the variances of these two data sets are not significantly different at the 5% level.

Thus, one can assume that in the case of the monthly average hourly values, all four components of net radiation measured at IAG and surface temperature measured at PEFI are representative of the urban area of São Paulo located inside the SRB domain (Fig. 1). A similar inference applies for monthly average hourly values of air temperature measured at IAG. The weaker regional representativeness of SW_{UP} is probably due to albedo differences between IAG rooftop and the urban area of São Paulo city.

It should be emphasized that the one-point (IAG) description of radiation balance components and radiometric properties given in the following Sections 4 and 5 will be considered as representative of the entire urban area of São Paulo city for monthly average hourly values as indicated by the representativeness analysis carried out above.

4 Radiation balance at the surface in the city of São Paulo

4.1 Diurnal variation

Figure 6 shows the diurnal variation of the monthly average hourly values of Q^* observed in the city of São Paulo during February and August of 2004. The amplitude of the diurnal cycle of Q^* in February is 562 Wm^{-2} and in August it is 524 Wm^{-2} (Table 7). During daytime, Q^* in February is systematically larger than in August. During the night, this

Table 6 Statistical parameters based on monthly average hourly values of the four components of surface radiation balance (SW_{DW}, SW_{UP}, LW_{DW}, LW_{UP}) and air and surface temperatures (T_{AIR}, T_{SUR})

Variable	N	MBE	RMSE	R^2	F	P
SW_{DW}	96	11.2 Wm^{-2}	45.2 Wm^{-2}	0.95	1.03	0.90
SW_{UP}	96	1.8 Wm^{-2}	10.2 Wm^{-2}	0.77	1.01	0.98
LW_{DW}	96	1.2 Wm^{-2}	8.6 Wm^{-2}	0.84	1.42	0.09
LW_{UP}	96	−11.1 Wm^{-2}	14.1 Wm^{-2}	0.89	0.89	0.56
T_{AIR}	288	0.56°C	1.02°C	0.89	0.96	0.70
T_{SUR}	288	−1.18°C	1.62°C	0.93	1.04	0.84

The columns indicate the number of values (N), the MBE, the RMSE, the R^2, and F and P values estimated from the variance test

MBE mean bias error, *RMSE* root mean standard error, R^2 determination coefficient

Q1

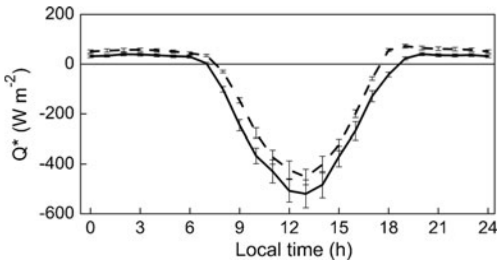

Fig. 6 Diurnal evolution of net radiation at the surface in the city of São Paulo during February (*solid line*) and August (*dash line*) in 2004. Statistical errors are indicated by *vertical bars*

pattern inverts, and Q^* in February becomes smaller than it is in August. Figure 7 and Table 7 indicate the diurnal variation of the monthly average hourly values of SW_{DW}, SW_{UP}, LW_{DW}, and LW_{UP} observed in the city of São Paulo during February and August of 2004. During the daytime, the net radiation is determined by shortwave radiation components, which in turn go through a minimum during the winter months (August), whereas during the nighttime, the low moisture content explains the maximum surface longwave emission observed during the winter months (mainly August).

4.2 Seasonal variation

The seasonal variation of the monthly average daily values of Q^*, SW_{DW}, SW_{UP}, LW_{DW}, and LW_{UP} are displayed in Fig. 8. The amplitude of net radiation in São Paulo is approximately equal to 7.27 MJ m^{-2} day^{-1}, with a maximum in December and a minimum in June (Table 7).

As expected for all components of the radiation balance at the surface, the monthly average daily values of SW_{DW} and SW_{UP} show the largest seasonal variation of 45% and 50%, respectively, with higher values in the spring (September) and lower values during the fall and winter (respectively May and June). In 2004, the amplitude of the annual cycle for daily values of SW_{DW} is 8.18 MJ m^{-2} day^{-1}, with a maximum in September and a minimum in May (Fig. 8 and Table 7). The annual cycle for daily values of SW_{UP} is 0.89 MJ m^{-2} day^{-1}, with a maximum also in September but the minimum in June. The seasonal variation of SW_{DW} in 2004 agrees with the one obtained from a longer period of observations (Oliveira et al. 2002). The only exception is the maximum in September. Both maxima observed for the daily value of SW_{DW} (and SW_{UP}) occurred in this month because the relative humidity and rain (and consequently cloudiness) were below climatological normal in São Paulo (Fig. 3). The minimum SW_{DW} in

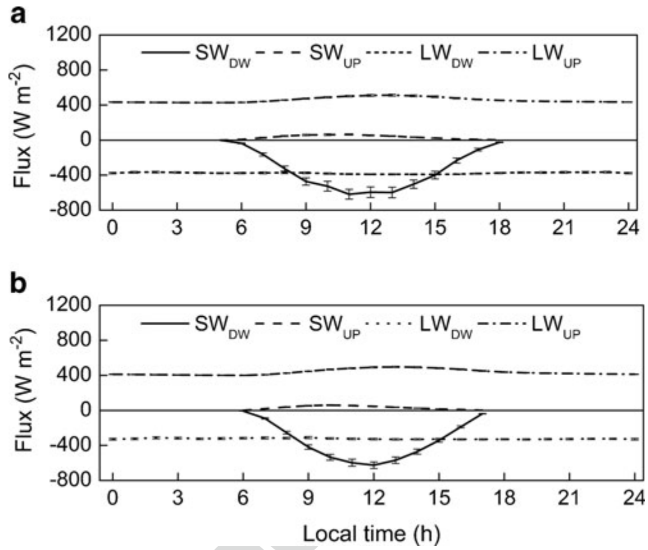

Fig. 7 Diurnal evolution of the components of the radiation balance at the surface in the city of São Paulo during **a** February and **b** August of 2004. Statistical errors are indicated by *vertical bars*

Table 7 Typical monthly average hourly and daily values of net radiation and its components making up the surface radiation balance for the city of São Paulo during 2004

Variable	Diurnal variation (W m^{-2})				Seasonal variation (MJ m^{-2} day^{-1})	
	February		August			
	Max	Min	Max	Min	Max	Min
Q^*	41±6	−520±56	72±8	−452±31	12.10±0.82 (December)	4.83±0.40 (June)
SW_{DW}	–	−643±60	–	−607±43	18.22±0.69 (September)	10.04±0.89 (May)
SW_{UP}	64±7	–	60±5	–	−1.79±0.08 (September)	−0.90±0.06 (June)
LW_{DW}	−377±8	−436±3	−329±9	−388±5	36.19±0.18 (January)	31.42±0.44 (July)
LW_{UP}	513±10	429±2	497±8	400±3	−39.63±0.35 (February)	−35.96±0.28 (July)
Radiometric parameters						
Broadband atmospheric transmissivity	0.46	0.22	0.60	0.28	0.57 (September)	0.36 (October)
Effective surface albedo	0.13	0.07	0.17	0.06	0.10 (April and September)	0.08 (June)
Effective atmospheric emissivity	0.93	0.88	0.83	0.76	0.92 (December and January)	0.79 (September)
Effective surface emissivity	0.98	0.96	0.99	0.94	0.97 (August)	0.95 (July)

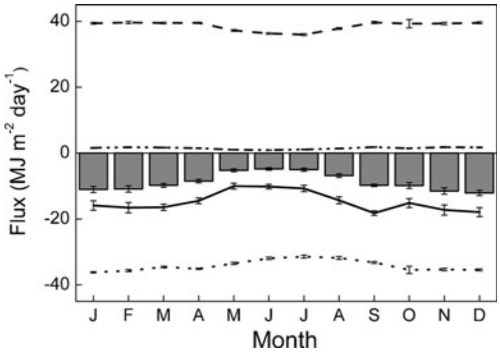

Fig. 8 Seasonal variation of the monthly average daily values of net radiation (*gray column*), incoming shortwave radiation (*solid line*), outgoing shortwave radiation (*dashed-dotted line*), incoming longwave radiation (*dotted line*), and outgoing longwave radiation (*dashed line*) at the surface in the city of São Paulo in 2004. Statistical errors are indicated by *vertical bars*

May is due to the high probability that cloudiness was above normal during this month in 2004 (Fig. 3).

The seasonal variation of longwave components of radiation in São Paulo is smaller than that of the shortwave components. The amplitude of the annual cycle is 4.77 MJ m^{-2} day^{-1}, indicating that the daily value of LW_{DW} in July is approximately 13% smaller than it is in January (Table 7). This reduction is due mainly to the seasonal variation in the air temperature (Fig. 3a). Another factor (which will be explored in the next section) is that in São Paulo, the effective atmospheric emissivity shows a maximum in the summer months and a minimum in the winter. This pattern is associated with the seasonal variation of moisture content of the atmosphere and cloudiness in São Paulo. The seasonal evolution of LW_{UP} is smaller than that of LW_{DW}. The amplitude of the annual cycle is 3.67 MJ m^{-2} day^{-1}, indicating that the daily value of LW_{UP} in July is about 9% smaller than it is in February (Table 7). This behavior reflects mainly the seasonal evolution of surface temperature in the city of São Paulo.

5 Radiometric properties of São Paulo city

Diurnal and seasonal variations of four radiometric properties were estimated for São Paulo city: broadband atmospheric transmissivity, surface effective albedo, and atmospheric and surface effective emissivity. Both emissivities are estimated by considering the air and surface temperatures to be representative of the urban area of São Paulo city, as indicated in Section 3.4.

5.1 Broadband atmospheric transmissivity

Figure 9 shows the diurnal variation of atmospheric broadband transmissivity (Γ) estimated in February (Fig. 9a) and in August (Fig. 9b) using monthly average hourly values of SW_{DW} observed in the city of São Paulo and monthly average hourly values of SW_{TOP} estimated according to Iqbal (1983). The amplitude of the diurnal cycle of Γ is the highest in August because the moisture content of the atmosphere and the cloudiness in São Paulo city are somewhat reduced in this month (Table 7). Figure 9c shows the seasonal variation of monthly average daily values of Γ, estimated from the monthly averaged daily values of SW_{DW} and SW_{TOP} The annual cycle of daily values of Γ has the highest value of 0.57 in September, a minimum of 0.36 in October, and a mean value of about 0.45. This seasonal pattern reflects mainly the variation in the moisture content of the atmosphere and cloudiness observed in 2004 (Fig. 3).

5.2 Effective surface albedo

The diurnal evolution of monthly average hourly values of effective surface albedo (α) in São Paulo is indicated in Fig. 10a, b for February and August. The hourly values of α shows the largest amplitude in August (Table 7). This behavior is due mostly to the seasonal variation in solar altitude. The asymmetry in α (Fig. 10a, b) is caused by a building effect on the SW_{UP} (Fig. 2b, c). The monthly averaged daily values of α indicate an annual variation of 20% in 2004, with the smallest value of 0.08 (June) and the

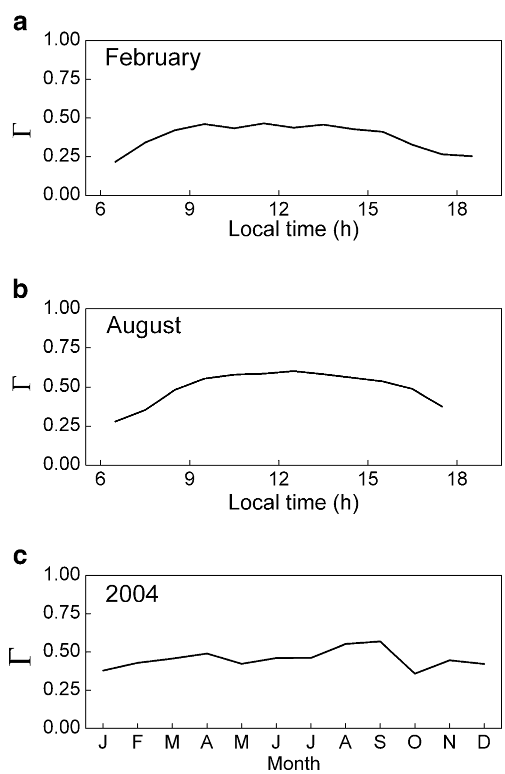

Fig. 9 Diurnal and seasonal variations of the atmospheric broadband transmissivity at the surface in **a** February, **b** August, and **c** 2004 at São Paulo

Q1

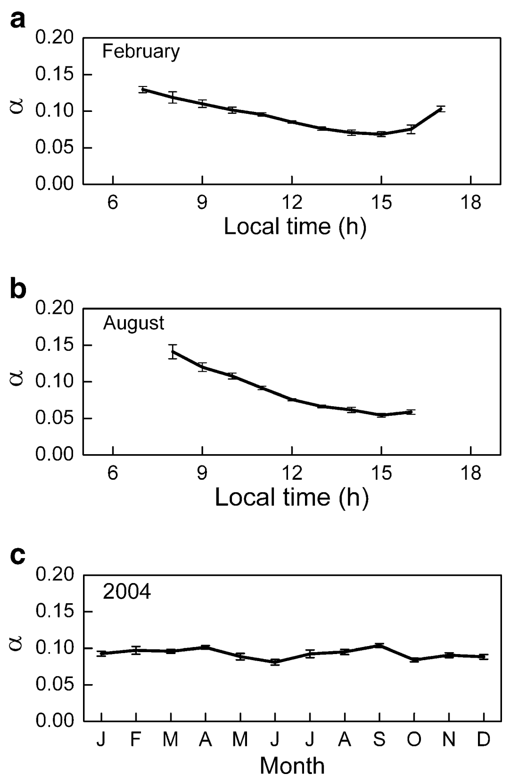

Fig. 10 Diurnal and seasonal variations of the surface effective albedo in **a** February, **b** August, and **c** 2004 at São Paulo. The *vertical lines* indicate statistical errors

largest value of 0.10 (April and September; Fig. 10c). This seasonal variation is associated with the combined vegetation and geometric effects. In the case of São Paulo, the two effects act in the opposite direction, canceling each other out during the year. The behavior of α in São Paulo is comparable to that found in other cities located at different latitudes (White et al. 1978; Vukovich 1983; Brest 1987; Oke 1988; Offerle et al. 2003), as displayed in Table 2.

5.3 Effective atmospheric emissivity

Figure 11a, b indicates the diurnal evolution of monthly average hourly values of atmospheric effective emissivity (ε_{ATM}) for São Paulo during February and August. The hourly values of ε_{ATM} are larger during February (Fig. 11a) due to a higher moisture content of the atmosphere during the summer months. In February, the amplitude of the diurnal cycle of ε_{ATM} in São Paulo is small. During summer, the contribution of clouds is distributed equally during the day, masking the diurnal cycle. However, in August (Fig. 11b), the diurnal cycle is well-defined, with a minimum during the daytime and a maximum during the nighttime. This behavior is related to the diurnal evolution of thermal stratification of the local UBL that reflects the low content of moisture typical of urban regions and the small cloud activity in the winter (Bárbaro et al. 2010). The monthly averaged daily values of ε_{ATM} (Fig. 11c) show a maximum of 0.92 (in December and January) and a minimum of 0.79 (in September). This oscillation is due to the seasonal evolution of air temperature, water vapor content, and cloudiness (Fig. 3).

5.4 Effective surface emissivity

Figure 12a, b shows diurnal evolution of the monthly average hourly values of the effective surface emissivity (ε_{SUR}) in São Paulo during February and August of 2004. The amplitude of the diurnal cycle of ε_{SUR} is slightly larger in August (about 1%) than it is in February. Figure 12c shows the seasonal variation of daily values ε_{SUR}. The daily values of ε_{SUR} show a seasonal variation of about 2% with a maximum value of 0.97 in August and a minimum of 0.95 in July (Table 7). Apparently, ε_{SUR} did not display diurnal or seasonal variations in 2004. These results indicate that the ε_{SUR} in São Paulo is not affected by land use variation due to the seasonal variation in vegetation and surface moisture as observed in other urban regions (Jin and Liang 2006). However, the values of ε_{SUR} estimated for São Paulo are comparable to those at other cities (Table 4) indicating that the effects associated to the material and geometry of the urban canopy are similar.

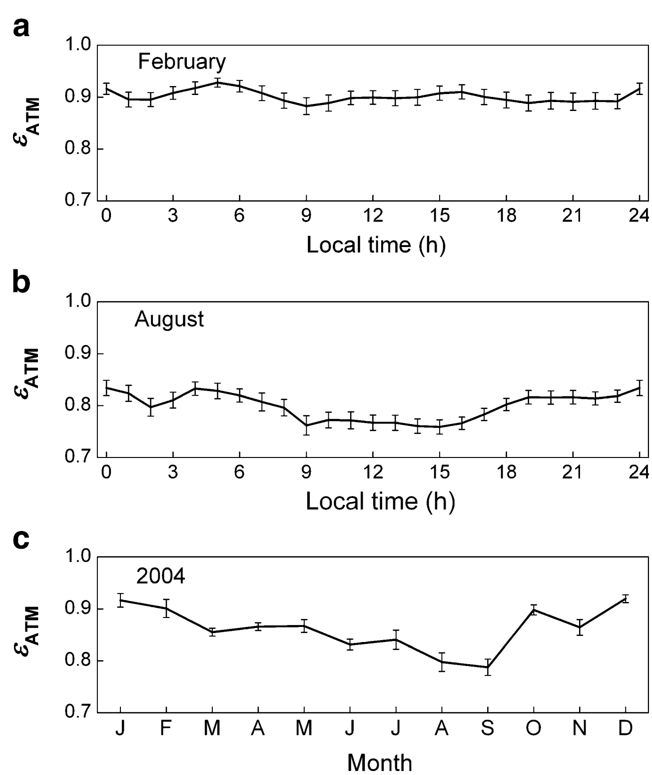

Fig. 11 Diurnal evolution and seasonal variation of the atmospheric effective emissivity at the surface in **a** February, **b** August, and **c** 2004 at São Paulo. The *vertical lines* indicate statistical errors

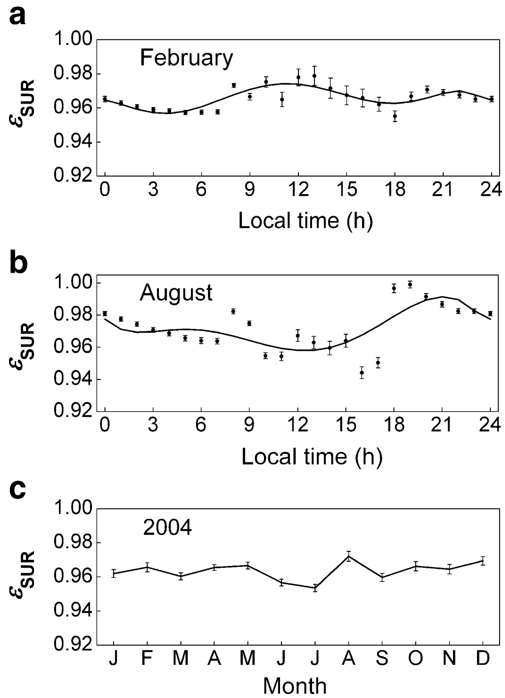

Fig. 12 Diurnal evolution of the surface emissivity during **a** February and **b** August and **c** seasonal variation at São Paulo. *Continuous lines* in **a** and **b** indicate the sixth-order polynomial fit. The *vertical lines* indicate statistical errors

6 Radiation balance and UHI in São Paulo

Urban effects in cities located at low latitude are less documented than in middle and high latitudes (Roth 2007; Arnfield 2003). The UHI in tropical and subtropical cities is less intense than in higher latitude cities, and it is more pronounced during daytime and strongly regulated by the moisture content of the atmosphere and soil in adjacent rural regions (Imamura 1991; Arnfield 2003; Roth 2007; Heisler and Brazel 2010). In the case of São Paulo, the urban effects on the temperature field have been investigated by several authors (Monteiro 1976, 1986; Lombardo 1984; Gonçalves et al. 2002; Pereira Filho et al. 2007; Freitas 2003). However, a clear picture of São Paulo UHI nature and intensity is not available so far. For instance, some authors believe that the UHI in São Paulo has a behavior typical of the middle latitude cities with maximum intensity during nighttime associated to the release of energy storage in the urban canopy and from anthropogenic Q6 sources (Monteiro 1976, 1986; Freitas et al. 2007). Other authors claim that the maximum intensity of UHI in São Paulo reaches as much as 12°C (Lombardo 1984; Monteiro 1986). On the other hand, more recent investigations have shown that the minimum value of air temperature in the city of São Paulo increased only about 2°C in the last 75 years as consequence of the urbanization, indicating that São Paulo city has much less intense impact in the local climate than indicated by the previous work (Gonçalves et al. 2002; Pereira Filho et al. 2007). Besides, according to Ferreira et al. (2011), the intensity of anthropogenic energy flux in the city of São Paulo has maximum amplitude of about 20 Wm^{-2}. This maximum occurs during daytime and it does not seem to be strong enough to sustain a nighttime UHI maximum in São Paulo, even during the winter when it represents as much as 15% of the daily value of the net radiation at the surface.

To clarify the nature and intensity of the UHI in the city of São Paulo, the diurnal evolution of UHI intensity was estimated for each month of 2004 as the difference between the urban and rural air temperature. Here, the difference is evaluated by the mean air temperature observed over the urban area of São Paulo city (using sites 1–9, Fig. 1) and by the mean temperature observed over the rural portion located at south of São Paulo city (sites 10–15, Fig. 1).

Contrarily to the previous works, the observations analyzed here indicate that the UHI in the city of São Paulo has a predominant daytime character, with a maximum intensity during afternoon (14:00–16:00 LT) and a minimum during morning time (07:00–08:00 LT) in almost all months of 2004. In January, November, and December, the minimum UHI intensity occurred at nighttime period (03:00–05:00 LT; Fig. 13a). The maximum intensity varied from 2.6°C in July (16:00 LT) to 5.5°C in September (15:00 LT) while the minimum intensity varied from −0.26°C (09:00 LT) in June to 0.94°C in November (03:00 LT).

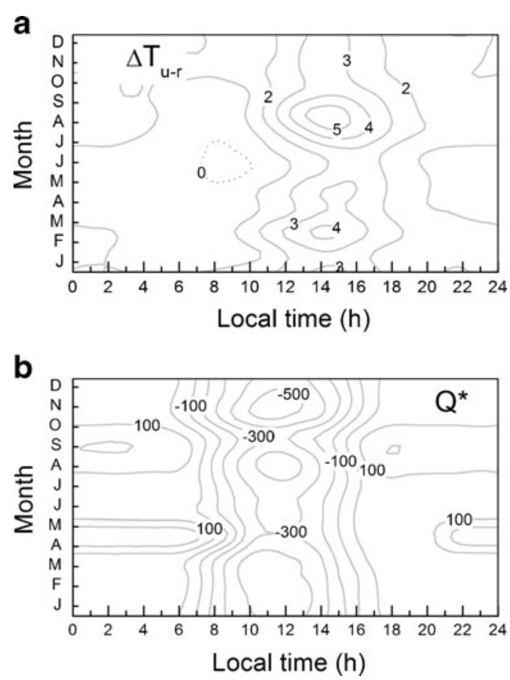

Fig. 13 Seasonal variation of the diurnal evolution of **a** UHI intensity (degree Celsius) and **b** net radiation (watts per square meter) at the surface in the city of São Paulo during 2004

These observations indicate also that the diurnal evolution of UHI intensity follows the diurnal evolution of the net radiation at the surface for all months of the year (Fig. 13b). In general, daytime UHI maximum occurs around 3 h after the maximum intensity of Q^* in 2004. The role played by the solar radiation in the UHI in São Paulo can be seen comparing the seasonal variation of monthly averaged daily values of net radiation, net longwave, and net shortwave (Fig. 14).

The UHI maximum intensity (5.5°C) occurs simultaneously to the net solar radiation maximum (September). Comparatively to the net solar radiation, the correlation between UHI and net radiation is less robust but still significant. The maximum net radiation happens during summer period (December, January, and February) when the UHI intensity is not a maximum.

To understand the net solar radiation, contribution to the UHI in São Paulo is necessary to consider the radiometric properties described in the previous section. The observations indicated that the albedo and emissivity of the surface in the urban area of São Paulo remains relatively constant during the entire year (respectively 0.09 and 0.96, Table 7). On the other hand, the atmospheric broadband transmissivity and effective emissivity show a significant seasonal variation. A maximum atmospheric broadband transmissivity (0.57) and a minimum atmospheric effective emissivity (0.79) occur simultaneously in September when the relative humidity reaches the minimum in São Paulo (73%) well below the climatological normal value (81%, Fig. 3b).

Comparatively to other months, in September arrives more solar radiation and leaves more longwave radiation. Assuming that the effective surface albedo is about 0.20 in rural areas near São Paulo urban region (Escobedo 2011, personal communication) and that the rural atmosphere emissivity value is unlikely to be smaller than its urban value, it is plausible to infer that there is a large inflow of energy in the urban canopy that yields a daytime UHI intensity of 5.5°C in September.

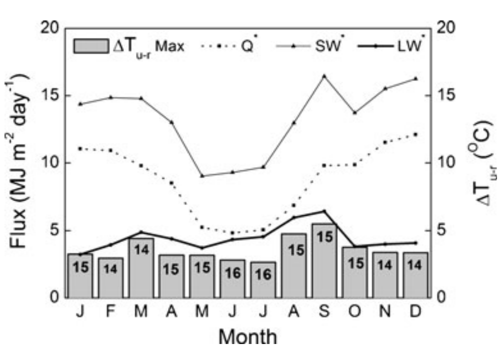

Fig. 14 Seasonal variation of the monthly average hourly value of maximum UHI intensity ($\Delta T_{u\text{-}r}$ max), monthly average daily values of net radiation (Q^*), net shortwave radiation (SW*), and net longwave radiation (LW*) at the surface in the city of São Paulo during 2004. The *numbers inside the gray columns* indicate time of the maximum $\Delta T_{u\text{-}r}$. Net radiation and net shortwave radiation are multiplied by −1

The inference described above assumed that the seasonal variation of the atmospheric broadband transmissivity over the rural areas is similar to the one observed over urban region. Similar considerations were carried out for other cities (Rouse et al. 1973; Peterson and Flowers 1977; Peterson and Stoffel 1980; Estournel et al. 1983; Oke 1988; Stanhill and Kalma 1995; Jáuregui and Luyando 1999; Christen and Vogt 2004; Giridharan et al. 2004; Rizwan et al. 2008).

7 Conclusions

The main objective of this work was to describe the diurnal and seasonal variations of the radiation balance at the surface in the city of São Paulo using in situ measurements of net radiation (Q^*) and its four radiation components (SW_{DW}, SW_{UP}, LW_{DW}, LW_{UP}) and air (screen level) and surface temperatures carried out during 2004.

A statistical analysis considering the MBE, the RMSE, the R^2, and a variance test between in situ measurements and estimates representative of large portions of urban region of São Paulo was carried out. The results show that one-point measurements are representative of the entire urban region for monthly average hourly values of SW_{DW}, SW_{UP}, LW_{DW}, LW_{UP} and air and surface temperature.

The seasonal variation of the monthly average hourly values indicated that the amplitudes of the diurnal cycles of Q^*, SW_{DW}, SW_{UP}, LW_{DW}, and LW_{UP} in February (the wettest month of summer in São Paulo) are 37%, 14%, 19%, 11%, and 5%, respectively, larger than they are in August (the driest month of the winter in São Paulo). The seasonal evolution of the monthly average daily values indicated a variations of 60% for Q^*, with a minimum in June and a maximum in December; 45% for SW_{DW}, with a minimum in May and a maximum in September; 50% for SW_{UP}, with a minimum in June and a maximum in September; 13% for LW_{DW}, with a minimum in July and a maximum in January; and 9% for LW_{UP}, with a minimum in July and a maximum in February.

Monthly average hourly and daily values of extraterrestrial solar radiation, SW_{DW}, SW_{UP}, LW_{DW}, LW_{UP} and air and surface temperature were used to estimate hourly and daily values of atmospheric broadband transmissivity (Γ), effective surface albedo (α), atmospheric effective emissivity (ε_{ATM}), and surface effective emissivity (ε_{SUR}). It was verified that Γ varies from 0.36 to 0.57, α from 0.08 to 0.10, and ε_{ATM} from 0.79 to 0.92, while ε_{SUR} remains approximately constant and equal to 0.96.

Based on patterns described above, one may conclude that, in addition to astronomical factors, the seasonal variations of Q^*, SW_{DW}, SW_{UP}, LW_{DW}, and LW_{UP} depend strongly on the seasonal variations of the radiometric properties of the atmosphere, mainly atmospheric broadband transmissivity and effective emissivity.

The seasonal variations of SW_{DW} and SW_{UP} depends more on the atmospheric broadband transmissivity and less on the surface effective albedo. In 2004, the maximum in the broadband transmissivity occurs in September as a result of the low moisture content of the atmosphere in São Paulo in this month.

The seasonal variations of LW_{DW} depend basically on the atmospheric effective emissivity while LW_{UP} reflects predominantly the seasonal variation of surface temperature. The maximum atmospheric effective emissivity occurs in September as a result of the low moisture content of the atmosphere in São Paulo in this month during 2004.

The values of radiometric properties of the atmosphere and the surface in the city of São Paulo agree with those reported from urban areas in Europe and North America. This indicates that the material and geometric configuration of the city of São Paulo do not differ much of the other cities. On the other hand, it was observed in 2004 that the UHI induced by São Paulo city varied between 2.6°C in July (at 16:00 LT) and 5.5°C in September at (15:00 LT). Contrarily to the previous work, the combination of the radiometric characteristics of the local atmosphere and surface result into a larger input of energy in the urban area of São Paulo generating UHI maximum intensity during daytime that is determined mainly by the seasonal variation of the daily values of the net solar radiation.

Acknowledgments The authors acknowledge the financial support provided by CAPES and CNPq (476.807/2007-7) and the set of data provided by project SRB at the NASA Langley Research Center Atmospheric Science Data Center. We thank Sebastião Antonio Silva and Samuel Reis Silva, Systems Analyst, and João Ricardo Neves for valuable assistance.

References

Adebayo YR (1990) Aspects of the variation in some characteristics of radiation balance within the urban canopy of Ibadan. Atmos Environ B24:9–17. doi:10.1016/0957-1272(90)90004-E

Arnfield AJ (2003) Two decades of urban climate research. A review of turbulence, exchanges of energy and water, and the urban heat island. Int J Climatol 23:1–26. doi:10.1002/joc.859

Balling RC, Brazel SW (1988) High-resolution surface-temperature patterns in a complex urban terrain. Photographic Eng Remote Sens 54:1289–1293

Bárbaro E, Oliveira AP, Soares J, Codato G, Ferreira MJ, Mlakar P, Božnar MZ, Escobedo FJ (2010) Observational characterization of the downward atmospheric longwave radiation at the surface in the city of São Paulo. J Appl Meteor Climatol 49(12):2574–2590. doi:10.1175/2010JAMC2304.1

Brest CL (1987) Seasonal albedo of an urban/rural landscape from satellite observations. J Appl Meteor 26:1169–1187. doi:10.1175/1520-0450(1987)026

CETESB (2009) Relatório da qualidade do ar no Estado de São Paulo 2008, CETESB, São Paulo, 2008, 167 pp. Available in Portuguese at http://www.cetesb.sp.gov.br/ar/qualidade-do-ar/31-publicacoes-e-relatorios.

Christen A, Vogt R (2004) Energy and radiation balance of a central European city. Int J Climatol 24:1395–1421

Codato G, Oliveira AP, Soares J, Escobedo JF, Gomes EN, Pai AD (2008) Global and diffuse solar irradiances in urban and rural areas in southeast of Brazil. Theor Appl Climatol 93:57–73. doi:10.1007/s00704-007-0326-0

Cohen B (2004) Urban growth in developing countries. A review of current trends and a caution regarding existing forecasts. World Dev 32(1):23–51. doi:10.1016/j.worlddev.2003.04.008

Collier CG (2006) The impact of urban areas on weather. Q J R Meteorol Soc 132:1–25. doi:10.1256/qj.05.199

Dalrymple GJ, Unsworth MH (1978) Longwave radiation at the ground. IV. Comparison of measurements and calculation of radiation from cloudless skies. Q J R Meteorol Soc 104:989–997. doi:10.1002/qj.49710444211

Diak GR, Mecikalski JR, Anderson MC, Norman JM, Kustas WP, Torn RD, Dewolf ERL (2004) Estimating land surface energy balances from space. Review and current efforts at the University of Wisconsin—Madison and USDA—ARS. Bull Amer Met Soc 85:65–78

Dousset B (1989) AVHRR-derived cloudiness and surface temperature patterns over the Los Angeles area and their relationship to land use. Proceedings of IGARSS-89 IEEE, New York, NY, pp 2132–2137

Escobedo JF, Gomes EN, Oliveira AP, Soares J (2011) Ratios of UV, PAR and NIR components to global solar radiation measured at Botucatu site in Brazil. Renew Energy 36:169–178. doi:10.1016/j.renene.2010.06.018

Estournel C, Vehil R, Guedalia D, Fontan J, Druilhet A (1983) Observations and modeling of downward radiative fluxes (solar and infrared) in urban/rural areas. J Appl Meteor Climatol 22:134–142. doi:10.1175/1520-0450(1983)022

Ferreira MJ (2010) Estudo do balanço de energia na superfície da cidade de São Paulo. Ph.D. thesis, Department of Atmospheric Sciences, University of São Paulo, São Paulo, Brazil, 183 pp. Available in Portuguese at: http://www.iag.usp.br/meteo/labmicro/publicacoes/Teses&Dissertacoes/index.html

Ferreira MJ, Oliveira AP, Soares J (2011) Anthropogenic heat in the city of São Paulo. Brazil Theor Appl Climatol 104:43–56. doi:10.1007/s00704-010-0322-7

Freitas ED (2003) Circulações locais em São Paulo e sua influência sobre a dispersão de poluentes. Ph.D. thesis, Department of Atmospheric Sciences, University of São Paulo, São Paulo, Brazil, 165 pp. Available in Portuguese at: http://www.teses.usp.br/teses/disponiveis/14/14133/tde-16032006-160700/pt-br.php

Garratt JR, Prata AJ (1996) Downwelling longwave fluxes at continental surfaces—a comparison of observations with GCM simulations and implications for the global land-surface radiation budget. J Climate 9:646–655. doi:10.1175/15200442(1996)009

Giridharan R, Ganesan S, Lau SSY (2004) Daytime urban heat island effect in high-rise and high-density residential developments in Hong Kong. Energy Build 36:525–534. doi:10.1016/j.enbuild.2003.12.016

Gonçalves FLT, Dias PLS, Araújo GP (2002) Climatological analysis of extreme low temperatures in Sao Paulo City, Brazil: impact of the oceanic SST anomalies. Int J Climatol 22(12):1511–1526. doi:10.1002/joc.764

Q1

Grimmond CSB (1992) The suburban energy balance. Methodological considerations and results for a mid-latitude west coast city under winter and spring conditions. Int J Climatol 12:481–497. doi:10.1002/joc.3370120506

Grimmond CSB, Souch C, Hubble MD (1996) Influence of tree cover on summertime surface energy balance fluxes, San Gabriel Valley, Los Angeles. Clim Res 6:45–57. doi:10.3354/cr0006045

Gupta SK, Ritchey NA, Wilber AC, Whitlock CH, Gibson GG, Stackhouse PW Jr (1999) A climatology of surface radiation balance derived from satellite data. J Climate 12:2691–2710. doi:10.1175/1520-0442(1999)012

Heisler GM, Brazel AJ (2010) The urban physical environment: temperature and urban heat islands. Am Soc Agronomy Agronomy Monogr 55:29–56. doi:10.2134/agronmonogr55.c2

Henry JA, Dicks SE, Wetterqvist OF, Roguski SJ (1989) Comparison of satellite, ground-based, and modeling techniques for analyzing the urban heat island. Photographic Eng Remote Sens 55:69–76

Hinkelman LM, Stackhouse PW Jr, Wielicki BA, Zhang T, Wilson SR (2009) Surface insolation trends from satellite and ground measurements. Comparisons and challenges. J Geophys Res 114:D00D20. doi:10.1029/2008JD011004

IBGE (2008) Demographics censuses. http.//www.ibge.gov.br/english/

Imamura IR (1991) Observational studies of urban heat island characteristics in different climate zones. Ph.D. dissertation, Inst. of Geoscience, University of Tsukuba, Japan, pp 156

Iqbal M (1983) An introduction to solar radiation. Academic, New York, p 390

Jáuregui E, Luyando E (1999) Global radiation attenuation by air pollution and its effects on the thermal climate in Mexico City. Int J Climatol 19:683–694. doi:10.1002/(SICI)1097-0088(199905)

Jin M, Liang S (2006) An improved land surface emissivity parameter for land surface models using global remote sensing observations. J Climate 19(12):2867–2881. doi:10.1175/JCLI3720.1

Jonsson P, Eliasson I, Holmer B, Grimmond CSB (2006) Longwave incoming radiation in the tropics. results from field work in three African cities. Theor Appl Climatol 85:185–201. doi:10.1007/s00704-005-0178-4

Kalnay E, Cai M (2003) Impact of urbanization and land-use change of climate. Nature 423:529–531. doi:10.1038/nature01649

Landsberg HE (1981) The urban climate. Academic, New York, p 271

Lombardo MA (1984) A ilha de calor da Metrópole Paulistana. Tese de Doutorado, Departamento de Geografia, Universidade de São Paulo, 270 pp (available in Portuguese)

Masson V (2006) Urban surface modeling and the meso-scale impact of cities. Theoretical Appl Climatol 84:35–45. doi:10.1007/s00704-005-0142-3

Mira M, Valor E, Boluda R, Caselles V, Coll C (2007) Influence of the soil moisture effect on the thermal infrared emissivity. Tethtys 4:3–9

Monteiro CAF (1976) Teoria e clima urbano In: Série Teses e Monografias, n.25. Instituto de Geografia, Faculdade de Filosofia, Letras e Ciências Humanas, Universidade de São Paulo, São Paulo, pp 181

Monteiro CAF (1986) Some aspects of the urban climates of tropical South America: the Brazilian contribution. In: Oke TR (ed) Urban climatology and its applications with special regard to tropical areas. WMO no. 652. World Meteorological Organization, Geneva, pp 166–198

Moriwaki R, Kanda M (2004) Seasonal and diurnal fluxes of radiation, heat, water vapor, and carbon dioxide over a suburban area. J Appl Meteor 43:1700–1710. doi:10.1175/JAM2153.1

Niemelä S, Räisänen P, Savijärvi H (2001) Comparison of surface radiative flux parameterizations. Part I: longwave radiation. Atmospheric Res 58:1–18. doi:10.1016/S0169-8095(01)00084-9

Offerle B, Grimmond CSB, Oke TR (2003) Parameterization of net all-wave radiation for urban areas. J Appl Meteor 42:1157–1173. doi:10.1175/1520-0450(2003)042

Oke TR (1974) Review of urban climatology, 1968–1973. WMO technical note no. 134, WMO no. 383. World Meteorological Organization, Geneva

Oke TR (1982) The energetic basis of the urban heat island. Q J R Meteorol Soc 108:1–24. doi:10.1002/qj.49710845502

Oke TR (1988) The urban energy balance. Prog Phys Geography 12:471–508. doi:10.1177/030913338801200401

Oke TR (2004) Initial guidance to obtain representative meteorological observations at urban sites. Instruments and Methods of Observation Programme IOM Rep. 81, WMO/TD No. 1250, pp 51

Oliveira AP, Escobedo JF, Plana-Fatori A, Soares J, Santos PM (1996) Medidas da radiação solar na cidade de São Paulo. Calibração de piranômetros e aplicações meteorológicas. Revista Brasileira de Geofísica 14:203–216

Oliveira AP, Escobedo JF, Machado AJ, Soares J (2002) Diurnal evolution of solar radiation at the surface in the City of São Paulo. Seasonal variation and modeling. Theor Appl Climatol 71:231–249. doi:10.1007/s007040200007

Oliveira AP, Bornstein R, Soares J (2003) Annual and diurnal wind patterns in the city of São Paulo. Water, Air and Soil Pollution: Focus 3:3–15. doi:10.1023/A:1026090103764

Pereira Filho AJ, Santos PM, Xavier TMB (2007) Evolução do tempo e do clima na região metropolitana de São Paulo, 1st edn. Linear B, São Paulo, 282 pp (available in Portuguese)

Peterson JT, Flowers EC (1977) Interactions between air pollution and solar radiation. Sol Energy 19:23–32. doi:10.1016/0038-092X(77)90085-8

Peterson JT, Stoffel TL (1980) Analysis of urban–rural solar radiation data from St. Louis, Missouri. J Appl Meteor 19:275–283. doi:10.1175/1520-0450(1980)019

Pinker RT, Laszlo I (1992) Modeling surface solar irradiance for satellite applications on a global scale. J Appl Meteor 31:194–211. doi:10.1175/1520-0450(1992)031

Rizwan AM, Dennis YC, Liu C (2008) A review on the generation, determination and mitigation of urban heat island. J Environ Sci 20:120–128

Roth M (2007) Review of urban climate research in (sub) tropical regions. International J Climatol 27:1859–1873. doi:10.1002/joc.1591

Rouse WR, Noad D, McCutcheon J (1973) Radiation, temperature and atmospheric emissivities in a polluted urban atmosphere at Hamilton, Ontario. J Appl Meteor 12:798–807. doi:10.1175/1520-0450(1973)012

Sailor DJ, Fan H (2002) Modeling the diurnal variability of effective albedo for cities. Atmos Environ 36:713–725. doi:10.1016/S1352-2310(01)00452-6

Sailor DJ, Lu L (2004) A top-down methodology for developing diurnal and seasonal anthropogenic heating profiles for urban areas. Atmos Environ 38:2737–2748. doi:10.1016/j.atmosenv.2004.01.034

Schmid HP, Cleugh HA, Grimmond CSB, Oke TR (1991) Spatial variability of energy fluxes in suburban terrain. Bound-Layer Meteor 54:249–276. doi:10.1007/BF00183956

Sellers P, Rasool S, Bolle HJ (1990) A review of satellite data algorithms for studies of the land surface. Bull Amer Met Soc 71:1429–1447. doi:10.1175/15200477(1990)-071

Snedecor GW, Cocharan WG (1989) Statistical methods, 8th edn. Iowa State University Press, Ames, p 503

Stackhouse PWJR, Gupta SK, Cox SJ, Chiacchio M, Mikovitz JC (2000) The WCRP/GEWEX surface radiation balance project release 2. An assessment of surface fluxes at 1 degree resolution. NASA Langley Technical Report Server

Stanhill G, Kalma JD (1995) Solar dimming and urban heating at Hong Kong. Int J Climatol 15:933–941. doi:10.1002/joc.3370150807

Trusilova K, Jung M, Churkina G (2009) On climate impacts of a potential expansion of urban land in Europe. J Appl Meteor Climatol 48:1972–1980. doi:10.1175/2009JAMC2108.1

UN (2007) World urbanization prospects the 2007 revision. United Nations Population Division, Department of Economic and Social Affairs, United Nations Secretariat, New York, p 244

Voogt JA, Oke TR (1997) Complete urban surface temperatures. J Appl Meteor 36:1117–1132. doi:10.1175/1520-0450(1997)036

Voogt JA, Oke TR (2003) Thermal remote sensing of urban climates. Remote Sens Environ 86:370–384. doi:10.1016/S0034-4257(03)00079-8

Vukovich FM (1983) An analysis of the ground temperature and reflectivity pattern about St. Louis, Missouri, using HCMM satellite data. J Appl Meteor Climatol 22:560–571. doi:10.1175/1520-0450(1983)022

Welch RM, Zdunkowski WD (1976) A radiation model of the polluted atmospheric boundary layer. J Atmos Sci 33:2170–2184. doi:10.1175/1520-0469(1976)033

White JM, Eaton FD, Auer AH (1978) The net radiation balance of the St. Louis metropolitan area. J Appl Meteor 17:593–599. doi:10.1175/1520-0450(1978) 017

Wilks DS (2006) Statistical methods in the atmospheric sciences, 2nd edn. Academic, New York, p 627

Yang F (2006) Parameterizing the dependence of surface albedo on solar zenith angle using atmospheric radiation measurement program observations. Sixteenth ARM Science Team Meeting Proceedings, Albuquerque, NM, March 27–31

AUTHOR QUERIES

AUTHOR PLEASE ANSWER ALL QUERIES.

Q1. Please check if the suggested running head was appropriate.
Q2. Please check if the affiliations were correctly presented.
Q3. Kindly check if Table 2 footnotes were correctly presented.
Q4. Please check if Tables 3–7 were correctly presented.
Q5. "…using general circulation model (CSU/GCM)" here was changed to "…using Colorado State University general circulation model". Please check if appropriate.
Q6. "Freitas et al. 2007" was cited here but not found in the reference list. Please provide complete bibliographic information.